

Influence of oxygen in a plasma nitriding process

A. M. MALISKA, P. EGERT, A. R. DE SOUZA,* C. V. SPELLER, A. N. KLEIN
Departamento de Engenharia Mecânica/LABMAT, Universidade Federal de Santa Catarina, 88040-900 Florianópolis-SC, Brazil

The influence of oxygen on the nitride layer formation on sintered steels was studied in a plasma nitriding reactor as a function of the gas mixture and sample composition. The nitride layers were characterized by metallographic and electronic microscopy techniques.

The thickness, composition and microstructure of the layer were determined for three gas mixtures (100% N₂, 75% N₂ + 25% H₂ and 90% N₂ + 10% H₂) in plain sintered iron in Fe–1.5% Si sintered alloy. The plasma chemistry was studied by optical spectroscopy and mass spectrometry as a function of the oxygen concentration in the atmosphere in the range 0–4%. It was observed that for low oxygen concentrations (O₂ ≤ 4%), the layer thickness remain practically unaltered for the mixtures containing hydrogen, whereas the layer obtained when H₂ was not used is completely damaged if oxygen is present in the gas mixture.

When the gas discharge is in a N₂–H₂ mixture, a loss of oxygen is detected by mass spectrometry. These results are correlated with the sample analysis, and the depletion of the oxygen is interpreted in terms of oxygen–hydrogen reactions.

1. Introduction

Plasma nitriding has been largely used in the metallurgical industries as an alternative to more conventional nitriding, such as gas nitriding, for the case hardening of steel [1, 2]. The plasma nitriding method is explained by several authors [3–7]. Typically, it is produced by an abnormal low pressure gas discharge in a N₂–H₂ gas mixture, where the workpiece is the cathode and the vacuum chamber wall is the anode itself, connected to ground. This process presents a series of advantages in relation to other conventional nitriding processes. It is worthy of note that there is no generation of pollutant residues, less gas and energy consumption, high repeatability of the process, and reduced cycle time.

In spite of the very good industrial results of this process, several questions remain unexplained, such as (1) the role of the different reactive species present in the gas discharge and (2) the impurity influence on the layer formation. For the first question, several theories based on experimental data have been proposed [8–10]. In relation to the second question, we did not find any literature references. Nevertheless, some workers [6–8] have given special attention to the gas purity as an important parameter and have used ultra pure gases (99.999%) in their experiments. In an industrial process, the gas purity can be an important economic limitation of the applicability of this method. Consequently, it is very important to determine the allowed purity limits of the gases in such a process, as well as the influence of the impurities on the plasma chemistry of the N₂–H₂ discharge. More-

over, since oxygen is an important atmospheric constituent, we can suppose that it constitutes the principal impurity present in nitriding reactors.

Our purpose in presenting this paper is to point out the influence of oxygen, present in all processes as an impurity, in the nitrided layer formation and plasma parameters. We present results of the influence of the oxygen introduced as impurity, on the electrical plasma parameters and gas temperature, obtained by optical spectroscopy. We also compare the plasma parameters with the nitride layer microstructure for oxygen concentrations ranging from 0 to 4% for three N₂–H₂ gas mixtures ([H₂] ≡ 25%, [H₂] ≡ 10% and [H₂] ≡ 0%).

2. Experimental procedure

In the present study the desired sintered alloys were produced using as a base material ASC 100.29 iron powder. Due to its high oxygen affinity, the alloying element, Si, was introduced into sintered steels through ferrosilicon powder with 14.5% Si, producing a final composition of Fe–1.5% Si. The test samples consist of cylinders of 10 mm height and 10 mm diameter, and were produced by conventional powder metallurgical processing. Mixing of the powders, including the addition of 0.6% zinc stearate for lubrication, was performed in a laboratory mixer. The samples were compacted at 600 MPa. For Fe–1.5% Si, sintering was performed in a laboratory furnace at 1200 °C for 2 h in an Al₂O₃ tube in ultrapure hydrogen atmosphere. In the case of pure iron, sintering was done at 1150 °C, for 2 h, in a pre-purified hydrogen atmosphere.

* Author to whom correspondence should be addressed.

The samples were nitrided in a plasma reactor constituted of a stainless steel cylinder with 30 cm inner diameter and 30 cm height. This vacuum chamber was pumped by a mechanical 10 h^{-1} backstream protected vacuum pump. The experimental set-up is presented in Fig. 1.

Before each nitriding run, the samples were cleaned by ultrasound for 10 min in acetone. Furthermore, to assure the complete desorption of surface impurities, they were subjected to a low pressure (0.666×10^2 Pa) glow discharge (in H_2 or Ar) during 15 min in the nitriding reactor.

The nitriding treatment was done for 2 h in a pulsed d.c. glow discharge at 3.999×10^2 Pa. We used three gas mixtures with hydrogen concentrations of 25, 10 and 0%, respectively. For each substrate composition and gas mixture, the samples were nitrided in conditions where the oxygen concentration was varied from 0 to 4%, while the total pressure and the nitrogen-hydrogen composition were kept constant. To control the sample temperature a thermocouple was placed directly in the substrate through a small hole. This temperature was correlated with the gas temperature of the luminescent region which was determined by spectroscopy analysis of the rotational structure of the $\text{N}^+(\text{B}) \rightarrow \text{N}^+(\text{X})$ electronic transition. For our experimental conditions, the rotational temperature, can be correlated with that of the plasma [11]. To do so, we have used a Jobin-Yvon HR640 monochromator, provided with a 1200 grooves/mm holographic grating and a photcounting system which allows resolution of the electronic-rotational emission lines of the $\text{N}_2^+(\text{B}, 0, \text{J}') \rightarrow \text{N}_2^+(\text{X}, 0, \text{J}'')$ transition. The inten-

sities are then used to determine the rotational temperature [11].

Simultaneous mass spectrometry analysis was used to monitor the plasma chemistry during the treatment time as well as to determine the influence of the oxygen on the radical concentrations (NH_x , N, NO, etc.) formed during the process in the discharge. The mass spectrometer was a VG-Quadrupole SXP 600, directly coupled to the plasma reactor through a position controlled probe, as shown in Fig. 1.

The microstructure and thickness of the nitrided layers were analysed by standard optical metallography techniques, scanning electron microscopy and energy dispersive X-ray microprobe analysis.

3. Results

3.1. Plasma nitriding parameters

In order to control the nitriding process, we have investigated the evolution of the electrical discharge parameters, such as the cathode voltage, the current density and the gas temperature, as a function of the oxygen concentration. Fig. 2 shows the general trend of these parameters, in the 75% N_2 -25% H_2 mixture, for O_2 concentrations varying from 0 to 4%. We observe that the current density is almost independent of the O_2 concentration. However, the cathode potential necessary to maintain the current at a constant value, corresponding to the desired value of the sample temperature, increased almost linearly with oxygen concentration. This variation is attributed to changes in the ion composition in the cathode region, which in turn leads to a change in the ion flux on the

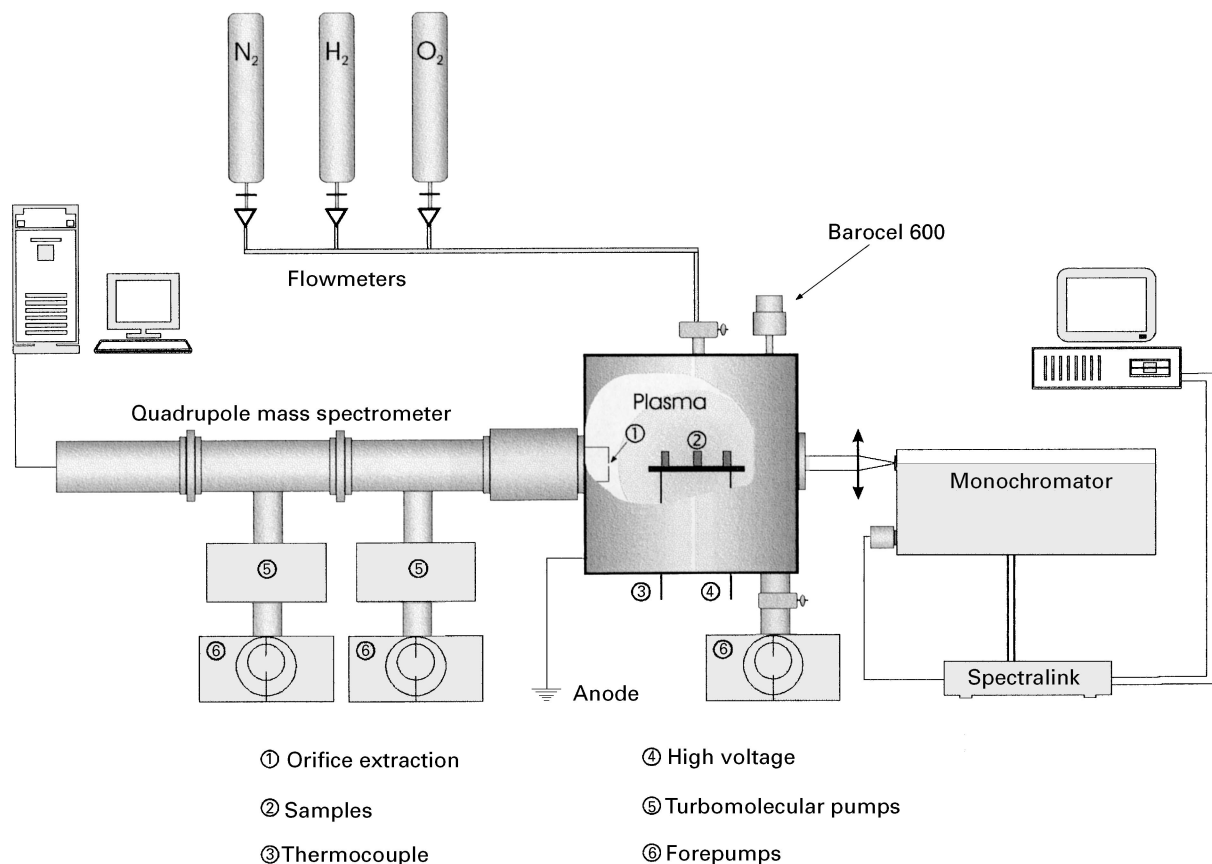


Figure 1 Schematic diagram of plasma nitriding apparatus.

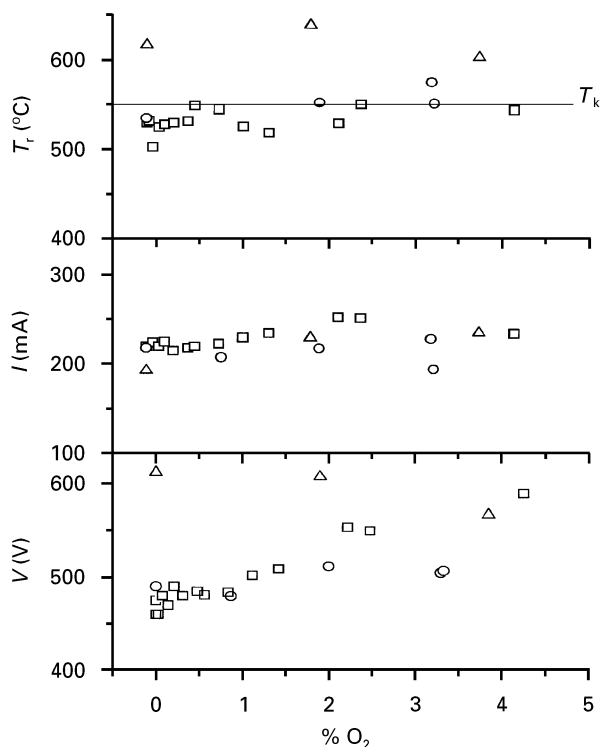
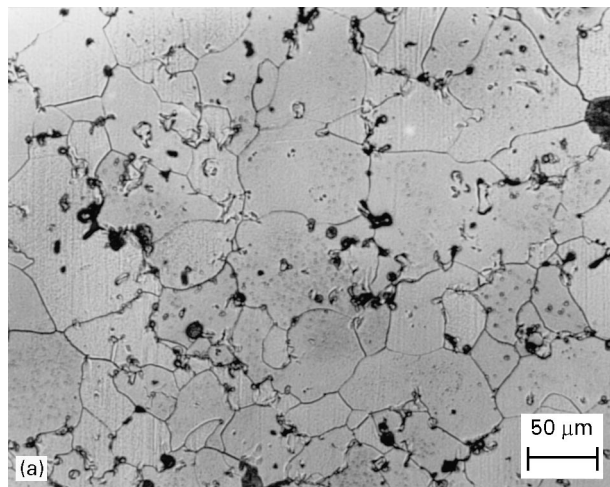


Figure 2 Current density, cathode voltage and rotational temperature as a function of oxygen concentration. \square 75% N_2 25% H_2 ; \circ 90% N_2 10% H_2 ; \triangle 100% N_2 .

sample surface. This fact will be the subject of future studies in our laboratory. Similar results were obtained for 90% N_2 –10% H_2 mixtures. However, for the discharge in pure N_2 , again the necessary potential to maintain the temperature at 550 °C had to be increased significantly. In addition, in accordance with reference [11], the rotational temperature could not be correlated with the sample temperature. It is important to emphasize that in these conditions the plasma is not always stable. For this reason, only three points were measured. It can be observed in Fig. 2 that, for hydrogen containing mixture, there is a very good correlation between the rotational temperature with the temperature measured using a thermocouple inserted directly into the sample.



3.2. Microstructural analysis of the samples

Due to the incomplete homogenization of alloying elements during the sintering process, sintered steels produced by powder mixture usually show a heterogeneous microstructure. Consequently, the microstructure of sintered samples show different phases, except in pure iron, which presents only a ferritic phase and pores, as shown in Fig. 3a. The microstructure of Fe–1.5% Si (Fig. 3b) can be considered almost totally ferritic with some pearlitic grains, due to the presence of carbon as an impurity (0.4%) in the ferro-silicon powder.

3.2.1. Plasma nitrated samples without oxygen addition

The heterogeneous microstructure influences the nitrated layer formation during the nitriding process. As already discussed by Maliska *et al.* [12], and as Fig. 4b clearly shows, there is a penetration of the compound layer through the boundaries of the original iron particles, which are enriched with silicon as a consequence of liquid phase formation and spreading (transient liquid phase sintering) of the Fe–Si alloy during the sintering process. This compound layer also surrounds those pearlites situated very close to the surface. The outermost pores, as well, are involved by the compound layer. In pure iron the layer also grows along open pores, but this effect is not so pronounced. The nitrated layer of pure iron samples showed a large amount of iron nitride needles well distributed in the diffusion zone, as shown in Fig. 4a. Despite the presence of these nitrated needles and small precipitates, the increase in the hardness in pure iron was very modest. It is speculated that the cause could be the large mean free path between those needles, and the non-existence of alloy nitrides.

For both pure iron and Fe–Si, the compound layer obtained in the two hydrogen–nitrogen containing gas mixtures is composed of a monolayer formed by ϵ and γ' phases, as detected in the X-ray diffraction profiles carried out on the surface of the treated samples. As for the case of treatment in pure nitrogen, the compound layer is composed of two different regions, as

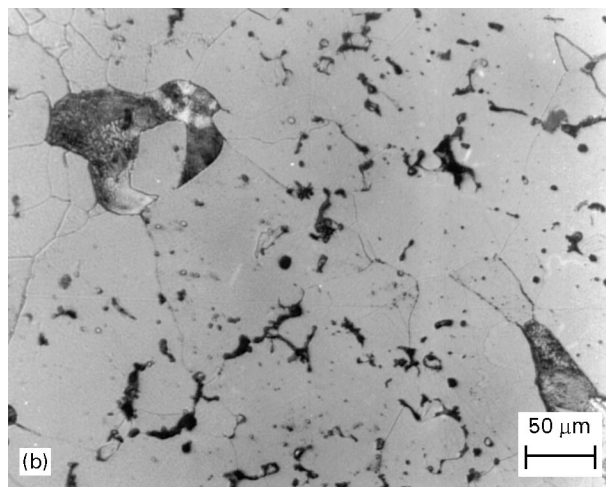


Figure 3 Optical micrograph of (a) sintered pure-Fe and (b) Fe–1.5% Si.

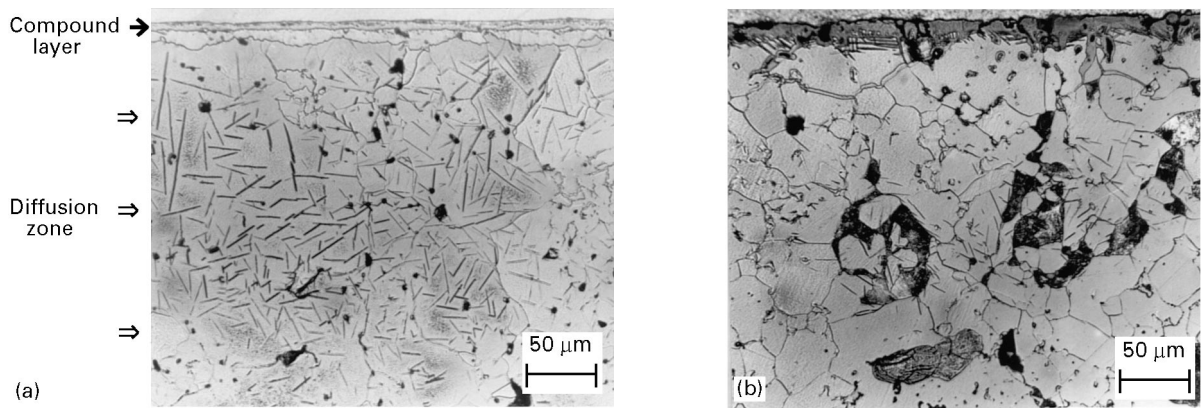


Figure 4 Optical micrograph of (a) pure-Fe and (b) Fe-1.5% Si nitrided for 2 h.

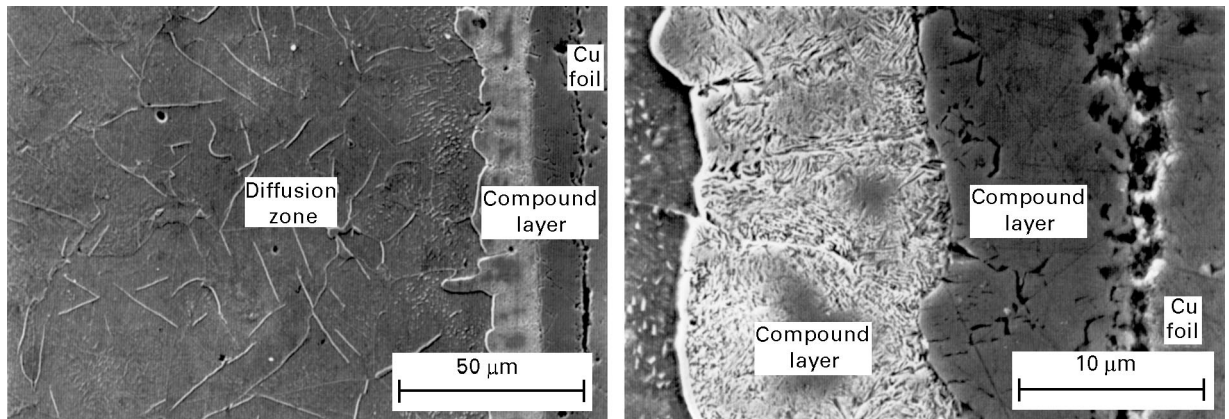


Figure 5 Electron microscopy of compound layer of pure iron plasma nitrided in 100% N₂.

can be seen in Fig. 5. In this case, the microprobe analysis has shown that the outermost region presents a high concentration of nitrogen.

3.2.2. Plasma nitrided samples with oxygen addition

The introduction of oxygen in the gas discharge caused no significant modification of the nitrided layer formed in the gas containing hydrogen. Tables I and II presents the main results and modifications produced in different experimental conditions.

Modifications that occurs in the nitrided layer due to impurity addition depends not only on the oxygen concentration but also on the N₂-H₂ mixture ratio. For the mixture with a high H₂ concentration, as is the case of 75% N₂-25% H₂, no modification of the nitride layer was observed up to 4.0% of O₂. In this mixture, the compound layer, as well as the diffusion layer, of the pure Fe and Fe-1.5% Si, showed the same metallographic characteristics as did the samples nitrided without O₂ addition. These results were corroborated by the energy dispersive spectroscopy (EDS) microprobe spectra obtained in those regions, which did not show any traces of oxygen. Even for higher impurity content, represented by 4.25% of O₂ (which corresponds to 20.0% of atmospheric air in the reactor), the presence of a thin oxide layer was only detected in the outermost region of the compound layer of

the pure Fe samples. This oxide layer was probably formed upon cooling the sample, when the discharge was off. In spite of this layer, all the remaining compound layer and the diffusion zone showed normal appearance, with abundant precipitation of nitride needles.

In the mixture 90% N₂-10% H₂, where the hydrogen content is lower, the oxygen addition caused few modifications in the nitrided layer for both alloys, as can be seen in Tables I and II. Only for an oxygen concentration higher than 3.0% (which corresponds to 15% of air), did the compound layer of pure iron show microstructural modification, with two distinct regions with different oxygen contents (Fig. 6). In this case, the compound layer was much more porous and fragile. For the Fe-1.5% Si sample, no microstructural modification of the nitrided layer was observed. Except for some traces of oxygen in the compound layer, detected in the EDS spectrum and which embrittle the compound layer, the compound layer as well as the diffusion zone showed the same metallographic aspect as that in the layer formed without oxygen.

For the mixture without H₂, the effect of the presence of oxygen during the plasma nitriding process is much more accentuated in the formation of the nitrided layer. Even for oxygen contents on the order of 2.0%, for the pure iron sample, the compound layer exhibits a double layer with higher oxygen content in

TABLE I Nitrided layer characterization of the pure Fe with impurity addition

| Mixture N ₂ /H ₂ | Impurity %O ₂ | Compound layer | | | Diffusion layer | | |
|---|-----------------------------|----------------|-----------------|----------------------------|-----------------|----------------------|----------------------------|
| | | Width (μm) | Characteristics | O ₂ presence | Width (μm) | Nitrides presence | O ₂ presence |
| 75/25 | 0.00 | 8.0 | mono | absent | 450 | abundant | absent |
| | 1.42 | 9.0 | mono | absent | 400 | abundant | absent |
| | 2.48 | 8.5 | mono | absent | 390 | abundant | absent |
| | 4.25 | 7.5 | mono | absent | 450 | abundant | absent |
| 90/10 | 0.00 | 6.0 | mono | absent | 350 | abundant | absent |
| | 0.67 | 8.0 | mono | absent | 400 | abundant | absent |
| | 2.00 | 7.5 | mono | absent | 500 | accentuated | absent |
| | 3.33 | 7.0 | double/fragile | accentuated | 450 | accentuated | absent |
| 100/00 | 0.00 | 14.0 | double | absent | 200 | abundant | absent |
| | 1.90 | 10.0 | double/fragile | accentuated | 250 | rare | present |
| | 3.85 | 13.5 | triple/fragile | accentuated | – | absent | present |

TABLE II Nitrided layer characterization of the Fe–1.5% Si alloy with impurity addition

| Mixture N ₂ /H ₂ | Impurity %O ₂ | Compound layer | | | Diffusion layer | | |
|---|-----------------------------|----------------|-----------------|----------------------------|-----------------|----------------------|----------------------------|
| | | Width (μm) | Characteristics | O ₂ presence | Width (μm) | Nitrides presence | O ₂ presence |
| 75/25 | 0.00 | 10.0 | mono | absent | 380 | normal | absent |
| | 1.42 | 10.0 | mono | absent | 340 | normal | absent |
| | 2.48 | 8.0 | mono | absent | 350 | normal | absent |
| | 4.25 | 9.0 | mono | absent | 360 | normal | absent |
| 90/10 | 0.00 | 10.0 | mono | absent | 380 | normal | absent |
| | 0.67 | 9.0 | mono | absent | 350 | normal | absent |
| | 2.00 | 10.0 | mono | absent | 340 | normal | absent |
| | 3.33 | 8.0 | mono/fragile | rare | 300 | normal | absent |
| 100/00 | 0.00 | 10.0 | mono | absent | 350 | normal | absent |
| | 1.90 | 8.5 | mono | absent | – | absent | absent |
| | 3.85 | – | absent | rare | – | absent | rare |

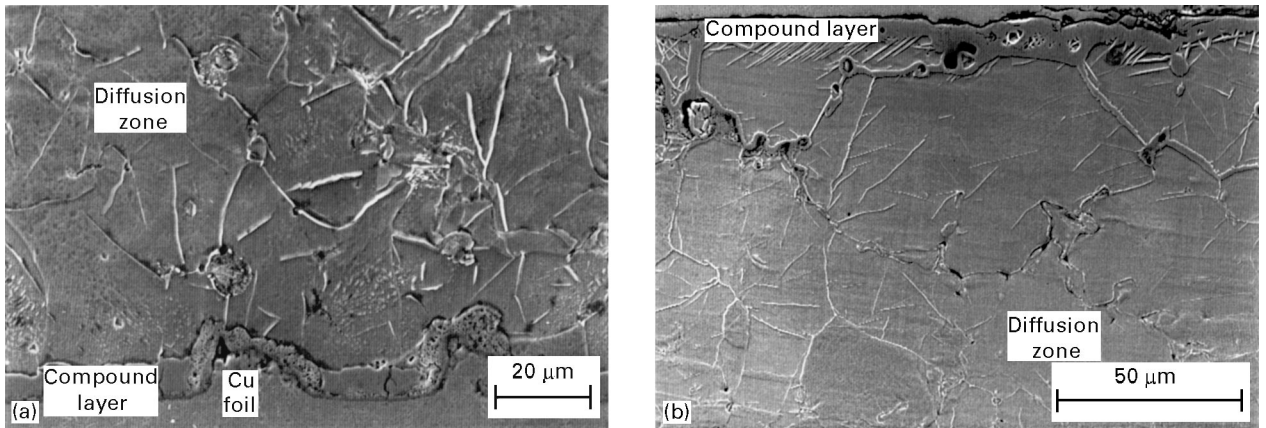


Figure 6 Electron microscopy microstructure of nitrided layer in mixture of 90% N₂–10% H₂ of (a) pure iron and (b) Fe–1.5% Si.

both regions, as can be seen in the spectrum of Fig. 7. This higher oxygen concentration makes the compound layer very fragile. The diffusion zone is also modified, with less precipitation of nitride needles and the presence of oxygen in the region close to the interface between the diffusion and the compound layer. For oxygen content over 3.0%, the brittleness of the compound layer is much more pronounced (Fig. 8a). In the case of Fe–Si alloy, for oxygen content up to 3.0% (Fig. 8b) no gradual modification of the nitrided layer was observed. Above that value, no compound layer was formed.

3.3. Plasma chemistry analysis

In order to determine the chemical identity of the different species in the glow discharge, a systematic study was done with the mass spectrometer, which allowed the determination of some of the neutral species. A summary of the results pertinent to this work, which were presented at the 47th Gaseous Electronics Conference [13], will be given here. The complete work on the subject shall be published elsewhere.

The species were sampled about 2 cm away from the substrate and it seems unlikely that they were formed on the sample surface. This was inferred from

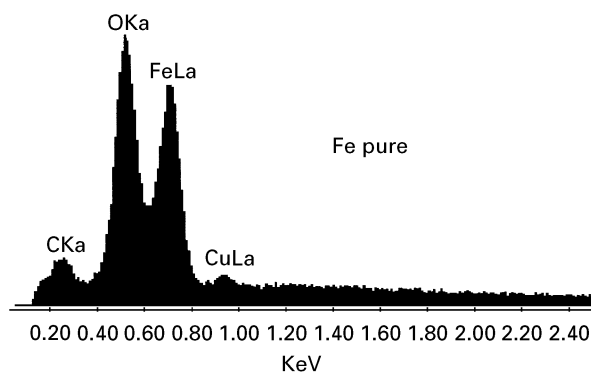


Figure 7 EDS spectra showing the oxygen peak of the compound layer of a pure iron sample, plasma nitrided in a nitrogen discharge with 2.0% of oxygen.

considerations on the species residence and lifetime under the experimental conditions used. Most species formed from reactions in the plasma surface region will preferentially exit the reactor (flow regime) rather than being collected by the sample orifice of the mass spectrometer. Therefore, the spectra obtained can be considered as representative of the discharge chemistry, which in principle excludes any strong perturbation from the nitriding process itself. The study of discharge chemistry during the nitriding process in our experiment only serves to establish a correlation between the gas discharge chemistry and the sample layer microstructure results. It is thus expected that a systematic determination of the chemical identity of the principal species will allow a better understanding of the physical chemistry involved in the nitriding process, as discussed in the next paragraph.

3.3.1. Formation of OH from H_2 and O_2

The mass spectrometric results presented hereafter can be summarized as follows: in a mixture of N_2-H_2 with traces of O_2 , the intensity of the peak corresponding to mass to charge ratio (m/z) = 17 (presumably OH^+ formed by ionization of radical OH) increases, while those of the peaks corresponding to m/z = 2 and 32 (identified as hydrogen and oxygen) decrease when the discharge is switched on. If hydrogen is not present in the mixture, the oxygen consumption is much less and a peak m/z = 30 (identified as NO) is formed.

Fig. 9a and b shows two spectra, for a 90% $N_2-10\% H_2$ mixture and for “pure” nitrogen, respectively, at a total pressure of 3.999×10^2 Pa and O_2 concentration of 1.3%. In order to interpret the results, a spectrum was always scanned before starting the discharge, which represented the initial neutral gas composition. Peaks with m/z = 17 and 18 correspond to ion fragments from the residual water (OH^+ and H_2O^+ , respectively) of the analysis chamber. For a given electron energy of the mass spectrometer ion source (70 eV in the present case), there will be a definite relative intensity between these two peaks, which, for the present purpose, we will call the “water reference”.

For the hydrogen containing spectrum (Fig. 9a), it was observed that, when the discharge was switched on, the relative intensity $I(17)/I(18)$ increased by about 33% above the “water reference” value. Since presumably $I(18)$ can correspond only to the residual water, and thus is supposed to be constant in the mass spectrometer chamber, new measurements were undertaken in order to identify the unknown species affecting the intensity corresponding to m/z = 17. Either another species with the same m/z as that for OH^+ (from H_2O) was being formed, or this same species was formed via another reaction mechanism (not from H_2O). Both alternatives would lead to an increase in the intensity of m/z = 17.

The presence of NH_3 , which yields NH_3^+ (m/z = 17) by direct ionization in the ion source, was confirmed by checking the appearance energy of the unknown species. However, it corresponds to a minor fraction of the observed difference, which means that at least one more species has to be considered in order to explain this difference. A strong candidate is OH^+ (second alternative given above), which would result from the direct ionization of OH.

The behaviour of the oxygen and the hydrogen peaks, m/z = 32 and m/z = 2, supports this assumption. Indeed, in addition to the increase of peak 17, a decrease of the relative intensities of $I(32)$ and $I(2)$ were readily observed in the spectra when the discharge was turned on. (All peaks are measured relatively to peak m/z = 28, which is related to nitrogen. Since nitrogen has a constant and well defined partial pressure, close to the total pressure value, it can be considered a good reference for all peaks.)

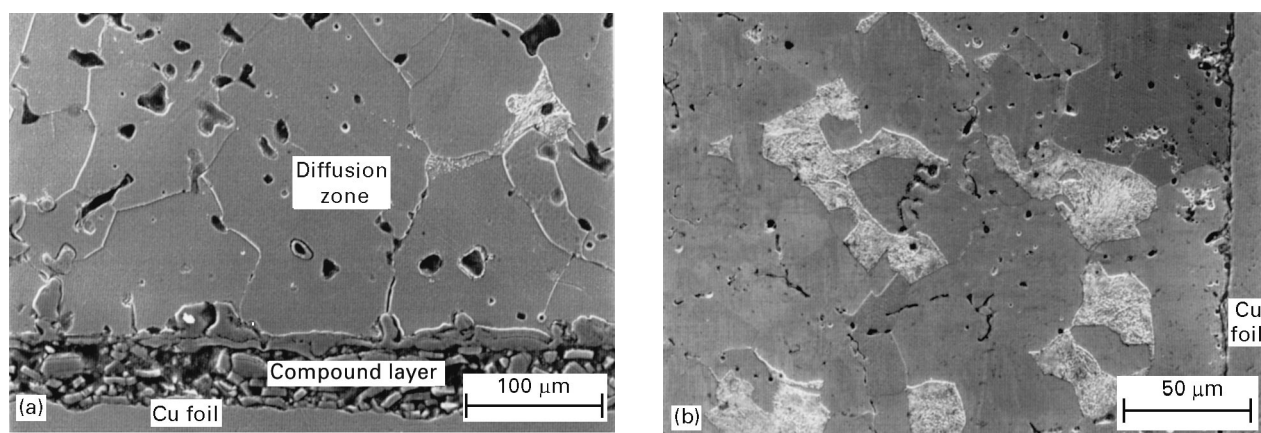


Figure 8 Electron microscopy of nitrided layer in pure nitrogen with 3.0% oxygen in (a) pure iron and (b) Fe-1.5% Si.

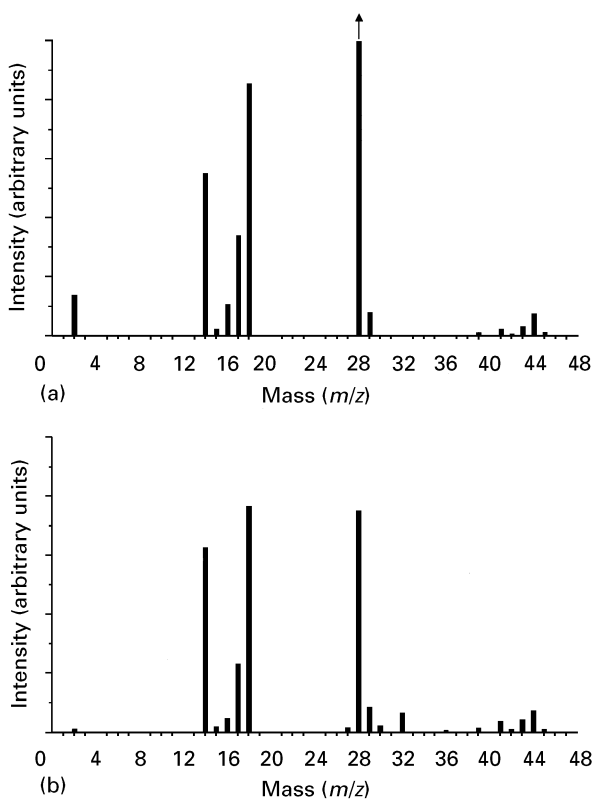


Figure 9 (a) Mass spectra of a 90% N_2 -10% H_2 mixture with 1.3% of added oxygen; (b) mass spectra of “pure” nitrogen with 1.3% of added oxygen.

For oxygen concentration above 1.3%, the relative concentration of $m/z = 17$ (OH^+ from OH) decreased continuously, becoming negligible for $[O_2] \gtrsim 4\%$ (for this concentration, it was only 1% above the “water reference”). These results seem to be correlated to those of the preceding section, where a relation was observed between the oxygen modification of the nitride layer and oxygen concentration for values larger than approximately 3–4%.

At this point it is important to point out that in pure nitrogen (Fig. 9b) the reduction of oxygen was much less important than in the presence of hydrogen (this can be inferred from comparison between spectra in Fig. 9a and 9b), which also suggests a relation between the presence of hydrogen and the loss of oxygen. Nevertheless, the relative intensity corresponding to $m/z = 30$ (presumably NO^+) increased, particularly when hydrogen was not present in the discharge, which suggests a second channel for oxygen consumption.

Finally, it was also observed that $m/z = 44$ (identified as CO_2^+ from CO_2) increased upon oxygen introduction in the mixture N_2-H_2 , for oxygen concentrations up to 4–5%. The correlation between the sample microstructure and the evolution of CO_2 is now under investigation in our laboratory.

The interpretation of the above results can be summarized as follows:

(a) If sufficient H_2 is present in the gas mixture, the concentration of oxygen introduced in the discharge decreases significantly (maximum of a factor of 4 in the present conditions) when the discharge is turned on.

(b) The reduction of oxygen is accompanied by a simultaneous reduction of hydrogen itself, while the intensities of the peaks 17 (identified as OH^+ from OH), 44 (identified as CO_2^+) and, in a lesser extent, 30 (identified as NO^+), increase.

4. Discussion

The presence of several radical species formed in the discharge during the nitriding process renders the chemical analysis of the plasma very complex. Although the initial gas mixture of N_2-H_2 is a relatively simple one before starting the discharge, the number of reactive species involved, neutral and ionic, can be very large during the time the discharge is on. In addition to the species formed in the “pure” mixture, contamination by O_2 or other gases such as CO_2 , from air or from wall degassing, can also contribute to an increase in the complexity of the chemistry, due to the formation of new reactive species. Finally, as we will see below, the chemical evolution of the plasma can induce electrical changes, which need to be controlled during the process.

In this section we will attempt to explain our experimental results on the basis of the plasma parameters and the layer characteristics.

4.1. Sample temperature

Regarding the electric potential and the current density, we can affirm that in our experiment the temperature is correlated with the current density, irrespective of the oxygen concentration over the experimental interval. In an abnormal glow discharge, the heating of the substrate sample is the result of its bombardment by ions accelerated in the cathode fall region (which corresponds roughly to 300–400 V in the present experimental conditions) as well as by rapid neutrals “heated” by charge transfer collisions in the cathode fall [14]. As explained in the preceding section, the cathode potential was varied in order to compensate any variation of the monitored temperature.

The decrease of the temperature as a function of the O_2 concentration can be tentatively explained by changes in ionic and neutral composition, which may result from charge transfer collisions. This probably modifies the potential sheath distribution in the cathode region, and thus the ion flux (current density); as for the second one, it will modify the “heated” neutral flux, thus also affecting the sample temperature. The same argument is valid for the effect of hydrogen on the temperature.

However, this variation does not affect the characteristics of the layer, provided the same current density (i.e. the same substrate temperature) is used.

It is important to note that either decrease of H_2 concentration or the increase of O_2 concentration leads to an increase of the characteristic potential. Either of these two changes can produce discharge instabilities which in turn will increase the arc probability in the different reactor parts, thus rendering more difficult the surface treatment. This behaviour is critical for a pure nitrogen discharge.

Another important result is related to the correlation of the rotational temperature (obtained by spectroscopy) with that of the sample (measured with a thermocouple). For the H₂-containing discharge, the two values are practically the same, but for pure N₂ or N₂ containing O₂, they are different. These results are consistent with those reported in reference [11], where the interpretation is given in terms of the kinetics of the N₂⁺ (B) state.

4.2. O₂ depletion

We have observed that the nitrided layer remains practically unaltered with oxygen addition if the gas discharge is produced in a N₂-H₂ mixture. These surprising results may be explained in terms of the plasma chemistry. For low oxygen concentration, the presence of oxygen was not detected in the samples and Fig. 9 allows us to explain this result. We observe a very important decrease of the oxygen concentration by the action of the gas discharge. The significant decrease of the oxygen concentration by the action of the hydrogen, prevents the layer oxidation. The apparent oxygen loss in the layer can be explained by reactions involving hydrogen in molecular or atomic states with atomic and molecular oxygen, probably producing OH. In fact, we have detected an increase of the peaks $m/z = 17$ and 18 (increase in 17 relatively larger than in 18), and a consequent decrease of the peak $m/z = 2$ corresponding to OH, H₂O and H₂, respectively. However, this mechanism remains to be verified and so is to be used with caution. The NO formation from N₂(X, $v > 13$) + O(³P) → N + NO ($v =$ vibration) is another path of oxygen depletion. Nevertheless, this reaction is not sufficient to explain our results, since we also observe the formation of NO in the pure-nitrogen discharge, but in this case the layer oxidation is very important. For a relatively high oxygen concentration (O₂ ≥ 4%), we have detected oxygen in the nitrided layer. This fact is probably due to the saturation of the reduction reactions. The layer is completely destroyed if no hydrogen is present in the gas mixture, even for low oxygen concentration.

In industrial processes, the economic aspects are very important. The level of oxygen impurity found in commercial gases should not affect the nitriding process and sophisticated vacuum system is not required. The limitations due to oxygen contamination can be ignored if we use a sufficient quantity of H₂ in the mixture.

5. Conclusions

Analysing the results on the addition of oxygen to the nitriding atmosphere for pure Fe and Fe-1.5% Si, we can point out some important conclusions about its effect on the nitrided layer.

1. The composition of the nitride layer due to the presence of oxygen in the nitriding process depends not only on the oxygen concentration, but also on the amount of hydrogen in the mixture, as well as on the elements present in the alloy.

2. The presence of hydrogen in the gaseous mixture prevents the prejudicial effect of oxygen in the formation of the nitrided layer. Mass spectrometric results strongly suggests that the radical OH is formed from hydrogen and oxygen in the discharge, thus contributing to neutralize the oxygen effect on the layer. Formation of CO₂ and NO could also contribute (to an unknown extent) to the depletion of oxygen.

3. In pure iron, increase of oxygen concentration in the mixture causes gradual microstructural modification of the nitrided layer. For alloys with high oxygen affinity elements (as is the case of Si), no gradual modification of the nitrided layer was observed as the concentration of oxygen was increased during the nitriding process. It disappeared in rather abrupt way.

4. Oxygen contamination is not a limiting factor in a plasma nitriding process provided the gas discharge is produced in N₂-H₂ mixtures (H₂ > 10%). For oxygen concentration of the order of 3% (which corresponds to 15% of air in the chamber) no influence on the layer was observed.

5. The potential characteristic of the cathode sheath may be modified to produce the same temperature for all gas mixtures. The temperature is the fundamental parameter to produce a good nitrided layer.

Finally, we can point out that we can use economical commercial gases to produce good nitrided layers, which is very important for industrial applications.

Acknowledgements

A. M. Maliska was supported by a grant from CNP_q/RHAÉ. P. Egert was supported by a grant from CNP_q.

References

1. T. SPALVINS in Proceedings of International Conference on Metallurgical Coatings, San Diego, CA (1983) p. 157.
2. B. EDENHOFFER, in "Heat Treatment of metals 2" (1974) p. 23.
3. C. K. JONES et al., "Ion nitriding, heat treatment" 73 (The Metal Society, London, 1975) p. 71.
4. P. C. JINDAL, *J. Vac. Sci. Technol.* **15** (1978) 313.
5. C. V. ROBINO and O. T. INAL, *Mater. Sci. Engng* **59** (1983) 79.
6. E. METIN and O. T. INAL, *J. Mater. Sci.* **22** (1987) 2782.
7. G. F. BOCCHINI, A. MOLINARI, B. TESI and T. BACCI, Metal Powder Report (1990) p. 772.
8. M. HUDIS, *J. Appl. Phys.* **44** (1973) 1489.
9. G. G. TIBETS, *ibid.* **45** (1974) 5072.
10. L. PETITJEAN and A. RICARD, *J. Phys. D: Appl. Phys.* **17** (1984) 919.
11. A. B. BRAND, J. L. R. MUZART and A. R. DE SOUZA, *J. Phys. D* **23** (1990) 1334.
12. A. M. MALISKA, A. R. SOUZA and A. N. KLEIN, *J. Surf. Coat. Technol.* **70** (1995) 175.
13. C. V. SPELLER, P. EGERT, A. R. DE SOUZA and J. L. MUZART, *Bull. Amer. Phys. Soc.* **39** (1994) 1453.
14. A. M. POINTU, in "Réactivité dans les plasmas (École d'Été d'Aussois, 1983)" (Les Editions de Physique, Les Ulis, France, 1984) p. 48.

Received 7 June 1995

and accepted 3 September 1996